Int. J. Solids Structures Vol 16, pp. 743–756

0020-7683/80/0801-0743/$02.00/0

BIFURCATION AND LIMIT POINT INSTABILITY OF DUAL EIGENVALUE THIRD ORDER SYSTEMS

P. SAMUELS
School of Information Science, Hatfield Polytechnic, Hatfield, Herts, England†

(*Received* 16 *March* 1979; *in revised form* 26 *November* 1979)

Abstract—In recent years, considerable effort has been devoted to the study of elastic structures buckling in two modes simultaneously. Provided there is not symmetry in both active co-ordinates, the associated potential function is essentially cubic in as much as it is this term which determines the post-buckling behaviour. The case of semi-symmetric potentials, where there is symmetry in just one of the co-ordinates, has been extensively studied by Thompson and Hunt. The general cubic potential with no symmetries has been investigated by the author while Ho proved that the worst failure of an imperfect cubic potential system occurs when the imperfection vector is in the direction of the perfect path of greatest slope. Further, she proved that this failure is by a limit point.

Here, a study is made of bifurcations and limit points arising in general third order systems and formulae are derived for their occurrence and for their corresponding failure loads. These are expressed in terms of certain trigonometric polynomials derived from the cubic part of the potential. These formulae are illustrated by consideration of a buckling model due to Thompson and Gaspar. We remove the symmetry so that a general third order potential system is obtained.

Finally, using a theorem of Bernstein on trigonometric polynomials, we provide an alternative and we think more intuitive proof of Ho's theorem.

1. INTRODUCTION

In investigating the buckling behaviour of a structural system at a two-fold branching point we must consider in the perfect case, the potential energy function

$$V(q_1, q_2, \lambda) = \frac{1}{2}\lambda \sum_{i,j=1}^{2} V_{ij}^{cc} q_i q_j + \frac{1}{6} \sum_{i,j,k=1}^{2} V_{ijk}^{c} q_i q_j q_k + \cdots \tag{1}$$

where q_1, q_2 are the two active co-ordinates, λ the change in load from the critical value and other notation is as in [1] and [2]. We do not assume semi-symmetry in the form of (1).

As discussed in [3], by changing to suitably normalised co-ordinates x and y the potential function (1) takes the form

$$V(x, y, \lambda) = -\frac{1}{2}\lambda(x^2 + y^2) + ax^3 + bx^2 y + cxy^2 + dy^3 + \cdots \tag{2}$$

and the origin becomes a geometric umbilic point of the energy surface in V–x–y space. In fact, the projections of the lines of curvature through the origin of this surface onto the x–y plane are precisely the post-buckling path tangent projections from λ–x–y space. These take the form $y = mx$ where m is a root of

$$cm^3 + (2b - 3d)m^2 + (3a - 2c)m - b = 0. \tag{3}$$

The perfect post-buckling paths in λ–x–y space are then given by

$$y = mx, \quad \lambda = (3a + 2bm + cm^2)x. \tag{4}$$

†This paper was written while the author was a visitor to the Department of Civil Engineering, University College London.

Following [1, 2], for the imperfect case we may suppose a potential function of the form

$$V(x, y, \lambda, \epsilon_1, \epsilon_2) = \epsilon_1 x + \epsilon_2 y - \frac{1}{2}\lambda(x^2 + y^2) + ax^3 + bx^2y + cxy^2 + dy^3 + \cdots \tag{5}$$

where ϵ_1 and ϵ_2 are major and principal imperfections in x and y respectively.

In [4], Ho used similar normalised co-ordinates to show that the lowest buckling load of an imperfect system occurs when the imperfection vector is in the direction of the perfect path of greatest slope and corresponds to a limit point. In Sections 2 and 3 we use such co-ordinates to show that bifurcations can only arise on imperfect paths as the intersection of a path in the plane of a perfect path and the λ-axis with a path in the plane determined by the other two perfect paths. This is strictly for the three path case but there are obvious modifications for the other cases, and it also shows that the semi-symmetric view of bifurcations in [1, 2], is quite general. We also confirm here the view of [3] that hill-top branching can only occur under the generalised spherical shell condition.

In Section 4 we use polar co-ordinates to enable us to express the potential function in terms of a trigonometric polynomial. Formulae for the occurrence and failure loads of limit points and bifurcations are then given in terms of these easily evaluated trigonometric polynomials. Examples are given showing how these formulae may be used:

Finally, we utilise a theorem of Bernstein on trigonometric polynomials to provide an intuitive proof of Ho's theorem.

2. BIFURCATIONS ON IMPERFECT PATHS

From (5), since imperfect paths are given by $(\partial V/\partial x) = (\partial V/\partial y) = 0$ they have equations

$$\lambda = \frac{3ax^2 + 2bxy + cy^2 + \epsilon_1}{x} = \frac{bx^2 + 2cxy + 3dy^2 + \epsilon_2}{y} \tag{6}$$

We note that $x = y = 0$ corresponds to $\lambda = -\infty$ and so in this way the imperfect path projections will all go through the origin in the xy-plane. Their equations are given by

$$cy^3 + (2b - 3d)y^2x + (3a - 2c)x^2y - bx^3 = \epsilon_2 x - \epsilon_1 y. \tag{7}$$

If m_i, m_j and m_k are the roots of (3) this may be written

$$c(y - m_i x)(y - m_j x)(y - m_k x) = \epsilon_2 x - \epsilon_1 y \tag{8}$$

We suppose that m_i is real but m_j and m_k may be either real or conjugate complex.

The imperfect paths are given by (6) as curves which are the intersection of two surfaces in λ–x–y space. There is a bifurcation on this path if the curve of intersection is itself the intersection of two space curves. This means that its projection (8) must be the intersection of two plane curves. Writing (8) as

$$c(y - m_i x)(y - m_j x)(y - m_k x) + \epsilon_i\left(y - \frac{\epsilon_2}{\epsilon_1}x\right) = 0 \tag{9}$$

if $\epsilon_i \neq 0$, we see that this can only occur if the imperfection vector is in the direction of one of the perfect post-buckling paths (it may point either way along it). The path projection then becomes

$$(y - m_i x)\{c(y - m_j x)(y - m_k x) + \epsilon_1\} = 0 \tag{10}$$

which is a combination of the plane paths

$$y - m_i x = 0, \quad c(y - m_j x)(y - m_k x) + \epsilon_1 = 0. \tag{11}$$

The two curves in (11) meet where

$$x^2 = \frac{-\epsilon_1}{c(m_i - m_j)(m_i - m_k)} \tag{12}$$

so that for a given imperfection vector in the direction m_i the sign of ϵ_i can be chosen so that bifurcation occurs. The equilibrium paths which project into (11) have equations

$$y = m_i x, \quad \lambda = (3a + 2bm_i + cm_i^2)x + \frac{\epsilon_1}{x} \tag{13}$$

and

$$c(y - m_j x)(y - m_k x) + \epsilon_1 = 0, \quad \lambda = 3ax + 2by + \frac{cy^2 + \epsilon_1}{x}. \tag{14}$$

It follows that the sign of x in (12) can always be chosen to ensure that the bifurcation occurs for negative λ corresponding to a change of stability at a load less than the critical load value for the perfect model. However, it may still not be an *initial* loss of stability for the imperfect system.

If m_j and m_k are real, the second curve in (11) is a hyperbola with the perfect post-buckling paths $y = m_j x$ and $y = m_k x$ as asymptotes. If m_j and m_k are conjugate complex this second curve is an ellipse. An alternative formulation of (14) is

$$c(y - m_j x)(y - m_k x) + \epsilon_1 = 0, \quad \lambda = 3ax + 2by + c(m_j + m_k)y - cm_j m_k x \tag{15}$$

on elimination of ϵ_1. We prove that the second part of (15) is the plane containing the perfect post-buckling paths $y = m_j x$ and $y = m_k x$. This will show that the semi-symmetric view of bifurcations of [1] and [2], as occurring via intersections of paths in the plane of a perfect post-buckling path and the λ-axis with those in the plane of the other two perfect post-buckling paths is true in general. These remarks are geometrically significant for the three path case but are algebraically correct when m_j and m_k are complex conjugate. When $m_j = m_k$ the plane in (15) contains the associated path.

For the proof we note that the plane containing the paths $y = m_j x$, $\lambda = (3a + 2bm_j + cm_j^2)x$ and $y = m_k x$, $\lambda = (3a + 2bm_k + cm_k^2)x$ has equation

$$\begin{vmatrix} x & y & \lambda \\ 1 & m_j & (3a + 2bm_j + cm_j^2) \\ 1 & m_k & (3a + 2bm_k + cm_k^2) \end{vmatrix} = 0$$

On expansion this gives

$$x(3am_j + 2bm_j m_k + cm_j m_k^2 - 3am_k - 2bm_j m_k - cm_j^2 m_k) - y(3a + 2bm_k + cm_k^2 - 3a - 2bm_j - cm_j^2) + \lambda(m_k - m_j) = 0$$

and hence

$$x(3a - cm_j m_k) + y(2b + c[m_j + m_k]) - \lambda = 0$$

which is the plane (15).

3. RELATIONSHIPS BETWEEN LIMIT POINTS AND BIFURCATIONS

The equilibrium path (13) is a hyperbola with the perfect path and λ-axis as asymptotes. We have

$$\frac{d\lambda}{dx} = (3a + 2bm_i + cm_i^2) - \frac{\epsilon_1}{x^2}, \quad \frac{d^2\lambda}{dx^2} = \frac{2\epsilon_1}{x^3} \tag{16}$$

so that for a suitable sign of ϵ_1 we have stationary points for positive and negative x of the same magnitude. For a maximum value, ϵ_1 and the perfect path slope $3a+2bm_i+cm_i^2$ have the same sign and x the opposite one. The equilibrium path (13) thus has a limit point at

$$x_i = \pm\left[\frac{\epsilon_1}{3a+2bm_i+cm_i^2}\right]^{1/2}, \quad \lambda_2 = -2\{\epsilon_1(3a+2bm_i+cm_i^2)\}^{1/2}. \tag{17}$$

It is already clear from (17) that an imperfection vector in a direction of a perfect path produces a lowest limit load in the direction of the one of steepest descent.

From Section 2 bifurcations can only occur when the imperfection vector is in the direction of a perfect post-buckling path. Further, in such cases they always occur for suitable choice of the sign of ϵ_1 even for negative λ. Hence it is in order, for such an imperfection direction, to compare the corresponding limit point and bifurcation failure loads. The bifurcation given by (12) being the intersection of paths (13) and (14) has

$$x_B = \pm\left[\frac{-\epsilon_1}{c(m_i-m_j)(m_i-m_k)}\right]^{1/2}, \quad \lambda_B = -(3a+2bm_i+cm_i^2)x_B - \frac{\epsilon_1}{x_B} \tag{18}$$

where the sign of x_B is chosen to ensure $\lambda_B < 0$.

When $c(m_i-m_j)(m_i-m_k)$ and $3a+2bm_i+cm_i^2$ have the same sign the limit point and bifurcation in the range $\lambda < 0$ appear on different paths (each path corresponding to a different sign of ϵ_1). When they have opposite sign they appear on the same path.

In all cases $\lambda_B^2 - \lambda_L^2 = [(3a+2bm_i+cm_i^2)x_B - (\epsilon_1/x_B)]^2 \geq 0$, so that for the same perfect path direction of imperfection vector and magnitude of ϵ_1, the corresponding bifurcation load is lower than the corresponding limit point load (these both occur for negative λ). This does not contradict Ho's theorem since the bifurcation may not correspond to an *initial* loss of stability. It turns out that in the case of the perfect path of steepest descent the corresponding bifurcation is never an initial loss of stability.

When the corresponding bifurcation and limit point appear on the same path the sizes of x_L and x_B determine which is the initial cause of failure. As shown in [1], [3] and [5], it is even possible for them both to coincide, when we have a hill-top branching point. This is the case when the spherical shell condition

$$b^2 + c^2 - 3bd - 3ac = 0 \tag{19}$$

is satisfied, see [3] and [6]. We can confirm this again since at a hilltop branching point $x_L = x_B$. This implies $3a+2bm_i+cm_i^2 = -c(m_i-m_j)(m_i-m_k)$. Using (3) we obtain $3a+2bm_i+2cm_i^2 = 3a-2c-2cm_jm_k$, which becomes $cm_i^2+bm_i+(c+cm_jm_k)=0$. By (3) again, if $m_i \neq 0$, $cm_i^3+bm_i^2+cm_i+b=0$ which leads to $c(m_i+(b/c))(m_i^2+1)=0$. Hence, for $m_i \neq 0$, $m_i = -(b/c)$. Substitution in (3) yields

$$b^3 + c^2b - 3db^2 - 3abc = 0. \tag{20}$$

If $b \neq 0$, this is the spherical shell condition (19), while if $b=0$ we are back to the case $m_i = 0$. In this exceptional case, we obtain $m_jm_k = -(3a/c)$, by equating x_L and x_B and $m_jm_k = (3a-2c)/c$ from (3). These together imply $c = 3a$ and hence (19) still holds.

Equation (19) is hence again seen to be the condition for a hill-top branching point in which the path in the plane determined by a perfect post-buckling path and the λ-axis is crossed at its limit point by a path in the plane determined by the other two paths. From [3], this can only occur in the homeoclinal case.

4. USE OF POLAR CO-ORDINATES AND TRIGONOMETRIC POLYNOMIALS

In polars, (2) takes the form

$$V(r,\theta,\lambda) = -\frac{1}{2}\lambda r^2 + r^3(a\cos^3\theta + b\cos^2\theta\sin\theta + c\cos\theta\sin^2\theta + d\sin^3\theta) + \cdots \tag{21}$$

where as usual $x = r\cos\theta$, $y = r\sin\theta$, $r \geq 0$ and $0 \leq \theta < 2\pi$.

For equilibrium$(\partial V/\partial r) = (\partial V/\partial\theta) = 0$ yielding

$$-\lambda r + 3r^2(a\cos^3\theta + b\cos^2\theta\sin\theta + c\cos\theta\sin^2\theta + d\sin^3\theta) = 0 \tag{22}$$

$$r^3(b\cos^3\theta + [2c-3a]\cos^2\theta\sin\theta + [3d-2b]\sin^2\theta\cos\theta - c\sin^3\theta) = 0\,. \tag{23}$$

Comparing (23) and (3) we see that the solutions of (23) are θ_i^1, θ_i^2, θ_j^1, θ_j^2, θ_k^1, θ_k^2 where $\tan\theta_n^1 = \tan\theta_n^2 = m_n$, $n = i, j, k$ and θ_n^1 and θ_n^2 differ by π. If $C(\theta) = a\cos^3\theta + b\cos^2\theta\sin\theta + c\cos\theta\sin^3\theta$ then (22) yields the perfect post-buckling paths as

$$\lambda = 3C(\theta_n^m)r, \quad n = i, j, k, \quad m = 1, 2\,. \tag{24}$$

Each path in the form (4) has been split into two paths in (24), each one starting at the origin.

$C(\theta)$, being a continuous function of θ, attains its extreme values over the range $0 \leqslant \theta \leqslant 2\pi$ and since $C(\theta)$ is everywhere differentiable and has period 2π, these extremes will be local ones. They will thus correspond to solutions of (23). Further, since $C(\theta+\pi) = -C(\theta)$, the values of θ which maximise and minimise $C(\theta)$ will be some θ_n^1 and θ_n^2 corresponding to the same m_n. They always exist whether (23) has two roots or six roots. From (24), the minimum and hence negative value of $C(\theta)$ corresponds to the perfect path of steepest descent.

In polars, (5) becomes

$$V(r, \theta, \lambda, \epsilon, \phi) = -\frac{1}{2}\lambda r^2 + r^3C(\theta) + \epsilon r\cos(\theta - \phi) \tag{25}$$

where $\epsilon_i = \epsilon\cos\phi$, $\epsilon_2 = \epsilon\sin\phi$, $\epsilon > 0$, $0 \leqslant \phi < 2\pi$. For equilibrium, $(\partial V/\partial r) = (\partial V/\partial\theta) = 0$ yielding

$$-\lambda r + 3r^2C(\theta) + \epsilon\cos(\theta - \phi) = 0 \tag{26}$$

$$r^3D(\theta) - \epsilon r\sin(\theta - \phi) = 0 \tag{27}$$

where $D(\theta) = b\cos^3\theta + (2c-3a)\cos^2\theta\sin\theta + (3d-2b)\cos\theta\sin^2\theta - c\sin^3\theta$. Equation (27) corresponds to (9) giving the imperfect path projections on the xy-plane, when coupled with $\lambda = 0$. Actually, (26) and (27) give the equilibrium paths as the intersection of two surfaces. (27) is a cylinder on the xy-plane projections and (26) is a surface with the property that each line parallel to the xy-plane and starting at the λ-axis either does not meet it or intersects it in two points exactly, possibly coincident. Now if the equilibrium path has a local extreme with respect to λ, then the plane parallel to the xy-plane through this extreme will touch the path at this point. Consequently so will the particular line in this plane joining this point to the λ-axis. As the equilibrium path is part of the surface (26), this line meets (26) in two coincident points and (26) has equal roots in r for the corresponding λ and θ. So at a limit point we have

$$\lambda_L^2 = 12C(\theta)\epsilon\cos(\theta - \phi), \quad r_L = \frac{\lambda_L}{6C(\theta)} = \left[\frac{\epsilon\cos(\theta-\phi)}{3C(\theta)}\right]^{1/2}. \tag{28}$$

Since we are interested in $\lambda < 0$, (28) shows that for an imperfect path to have a limit point in this range we must have $C(\theta) < 0$ and the imperfection direction ϕ chosen so that $\cos(\theta - \phi) < 0$. It further shows that the lowest limit load λ_L^* occurs at the θ_n^{m*} yielding the minimum $C(\theta)$ over the interval $[0, 2\pi]$ with direction of imperfection $\phi = \theta_n^{m*} + \pi$. So the lowest limit load occurs when the imperfection is in the direction of the perfect path of steepest descent, as shown by Ho[4]. For this lowest load

$$\lambda_L^{*2} = -12C(\theta_n^{m*})\epsilon, \quad r_L^* = \frac{\lambda_L^*}{6C(\theta_n^{m*})} = \left[\frac{-\epsilon}{3C(\theta_n^{m*})}\right]^{1/2}. \tag{29}$$

We need to check that this lowest load does always correspond to an initial loss of stability.

Trigonometric polynomials

A trigonometric polynomial is an expression of the form

$$\sum_{r=0}^{n} \{a_r \sin r\theta + b_r \cos r\theta\} \tag{30}$$

and n is its degree.

It is easy to see that $C(\theta)$ is a trigonometric polynomial of degree three. Consequently so are all of its derivatives. In what follows we will need to calculate $C(\theta)$ and its second derivative $E(\theta)$ for various θ. We shall need the expressions

$$C(\theta) = \frac{a-c}{4}\cos 3\theta + \frac{b-d}{4}\sin 3\theta + \frac{3a+c}{4}\cos\theta + \frac{3d+b}{4}\sin\theta \tag{31}$$

$$E(\theta) = \frac{9(c-a)}{4}\cos 3\theta + \frac{9(d-b)}{4}\sin 3\theta - \frac{(3a+c)}{4}\cos\theta - \frac{(3d+b)}{4}\sin\theta. \tag{32}$$

5. CRITICAL LOADS INCLUDING BIFURCATIONS

At a loss of stability,

$$\begin{vmatrix} V_{rr} & V_{r\theta} \\ V_{\theta r} & V_{\theta\theta} \end{vmatrix} = 0. \tag{33}$$

Further, with $E(\theta)$ as defined in the last section,

$$\begin{aligned} V_{rr} &= -\lambda + 6rC(\theta) \\ V_{\theta r} &= 3r^2 D(\theta) - \epsilon \sin(\theta - \phi) \\ V_{\theta\theta} &= r^3 E(\theta) - \epsilon r \cos(\theta - \phi). \end{aligned} \tag{34}$$

If we confine ourselves to the cases $\theta = \theta_n^m$, $n = i, j, k$, $m = 1, 2$ and $\theta - \phi = 0, \pm\pi$, then by Section 2 this includes bifurcations and from Section 4 this includes the lowest limit load. These conditions imply $V_{\theta r} = 0$ so (33) gives

$$[-\lambda + 6rC(\theta_n^m)][r^3 E(\theta_n^m) - \epsilon r \cos q\pi] = 0, \quad q = 0, 1$$

so either

$$r = \frac{\lambda}{6C(\theta_n^m)} \tag{35}$$

or

$$r^2 E(\theta_n^m) = \epsilon \cos q\pi. \tag{36}$$

Under (35), when $V_{rr} = 0$, we must have a limit point by comparison with (28). Further, it is also clear that we must have $q = 1$. For (35) to give an initial loss of stability, we require $V_{\theta\theta} \geq 0$. If θ_n^m corresponds to a negative minimum of $C(\theta)$, then $E(\theta_n^m) \geq 0$ and hence $V_{\theta\theta}$ is positive. Such θ_n^m hence ensure an initial loss of stability and in particular, it follows that the lowest limit load always occurs at an initial stability loss. A limit point at some θ_n^m and negative λ may not be an initial loss of stability when $C(\theta)$ is a negative maximum value. A hill-top branching point, being both a limit point and bifurcation, necessitates both stability coefficients V_{rr} and $V_{\theta\theta}$ being zero. These distinctions will be illustrated in the examples where it will be shown that negative maximum values of $C(\theta)$ can correspond, when $q = 1$, to initial failure by either limit point or bifurcation.

Our restriction to the cases $\theta = \theta_n^m$ allows us to consider only equilibrium paths in the plane determined by the λ-axis and the line $\theta = \theta_n^m$. Equation (35) has dealt with limit points on such paths when $C(\theta_n^m)$ is negative and $q = 1$. Equation (36) deals with bifurcations on such paths.

Under (36), when $V_{\theta\theta} = 0$, we have the condition for a bifurcation on these paths. It is immediate from (36) that a path corresponding to a negative minimum value of $C(\theta)$ and $q = 1$ has no bifurcation on it as $E(\theta) \geq 0$. We list the possible limit points and bifurcations in terms of properties of $C(\theta_n^m)$.

(I) $C(\theta_n^m)$ *is a positive minimum* (*both* $C(\theta_n^m)$ *and* $E(\theta_n^m)$ *positive*)

Bifurcations occur on an associated path with $q = 0$ but these always correspond to positive λ.

(II) $C(\theta_n^m)$ *is a positive maximum* ($C(\theta_n^m) > 0$, $E(\theta_n^m) < 0$)

There is a bifurcation on an associated with $q = 1$. The corresponding λ may or may not be negative.

(III) $C(\theta_n^m)$ *is a negative minimum* ($C(\theta_n^m) < 0$, $E(\theta_n^m) > 0$)

There is a limit point only on the associated path with $q = 1$. The path with $q = 0$ has a bifurcation which may or may not correspond to negative λ. However, in all cases, either this path or that in (II) does correspond to negative λ. But this bifurcation never corresponds to an initial loss of stability. To see this, substitute $r = [(\epsilon/E(\theta_n^m))]^{1/2}$ into equation (34) for V_{rr} to obtain

$$V_{rr} = \left[\frac{\epsilon}{E(\theta_n^m)}\right]^{1/2} (3C(\theta_n^m) - E(\theta_n^m))$$

which is negative.

(IV) $C(\theta_n^m)$ *is a negative maximum* (*both* $C(\theta_n^m)$ *and* $E(\theta_n^m)$ *negative*)

There is always both a limit point and bifurcation on the associated path with $q = 1$. Either of these may produce the initial los of stability or they may both coincide.

6. AN EXAMPLE

In order to illustrate these ideas we consider a variation of the buckling model presented by Thompson and Gaspar[8]. The model, shown in Fig. 1, consists of a light rigid strut of length L carrying a vertical load P. Support is provided by three linear springs initially inclined at 45° to the horizontal plane, one in the yz-plane and the others in vertical planes making angles α and $-\beta$ with the yz-plane.

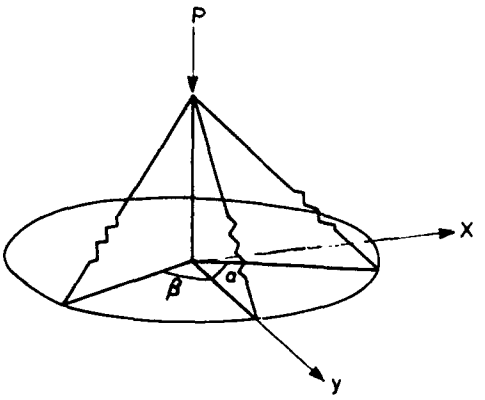

Fig. 1. A view of the buckling model.

Following Thompson and Gaspar in [8], the state of the structure can be specified by non-dimensional generalized co-ordinates u_1 and u_2 where

$$u_1 = \frac{x}{L} \quad \text{and} \quad u_2 = \frac{y}{L}$$

and (x, y) are the co-ordinates of the top of the strut.

We consider a family of imperfect systems characterised in the unloaded state by $u_1 = u_1^0$ and $u_2 = u_2^0$.

The extension of a general spring at horizontal angle ϕ is

$$\begin{aligned} e(\phi, u_1, u_2) = L\{&[(\sin\phi - u_1)^2 + (\cos\phi - u_2)^2 + 1 - u_1^2 - u_2^2]^{1/2} \\ &- [(\sin\phi - u_1^0)^2 + (\cos\phi - u_2^0)^2 + 1 - (u_1^0)^2 - (u_2^0)^2]^{1/2}\}. \end{aligned} \tag{37}$$

If c_1, c_2 and c_3 are the spring stiffnesses the strain energy in a deformed state is

$$U = \frac{1}{2}c_1 e^2(0, u_1, u_2) + \frac{1}{2}c_2 e^2(\alpha, u_1, u_2) + \frac{1}{2}c_3 e^2(-\beta, u_1, u_2). \tag{38}$$

The deflection of the load is

$$\epsilon = L[1 - (1 - u_1^2 - u_2^2)^{1/2}]. \tag{39}$$

The total potential energy function is $V(u_1, u_2, P) = U - P\epsilon$.

$$\begin{aligned} V(u_1, u_2, P) = L^2\Big[&u_1^2\Big(\frac{1}{4}c_2\sin^2\alpha + \frac{1}{4}c_3\sin^2\beta\Big) + u_2^2\Big(\frac{1}{4}c_1 + \frac{1}{4}c_2\cos^2\alpha + \frac{1}{4}c_3\cos^2\beta\Big) \\ &+ u_1u_2\Big(\frac{1}{2}c_2\sin\alpha\cos\alpha - \frac{1}{2}c_3\sin\beta\cos\beta\Big) + u_1^3\Big(\frac{1}{8}c_2\sin^3\alpha - \frac{1}{8}c_3\sin^3\beta\Big) \\ &+ u_1^2u_2\Big(\frac{3}{8}c_2\sin^2\alpha\cos\alpha + \frac{3}{8}c_3\sin^2\beta\cos\beta\Big) \\ &+ u_1u_2^2\Big(\frac{3}{8}c_2\sin\alpha\cos^2\alpha - \frac{3}{8}c_3\sin\beta\cos^2\beta\Big) \\ &+ u_2^3\Big(\frac{1}{8}c_1 + \frac{1}{8}c_2\cos^3\alpha + \frac{1}{8}c_3\cos^3\beta\Big) + u_1^0u_1\Big(-\frac{1}{2}c_2\sin^2\alpha - \frac{1}{2}c_3\sin^2\beta\Big) \\ &+ u_2^0u_2\Big(-\frac{1}{2}c_1 - \frac{1}{2}c_2\cos^2\alpha - \frac{1}{2}c_3\cos^2\beta\Big) \\ &+ u_1^0u_2\Big(-\frac{1}{2}c_2\sin\alpha\cos\alpha + \frac{1}{2}c_3\sin\beta\cos\beta\Big) \\ &+ u_2^0u_1\Big(-\frac{1}{2}c_2\sin\alpha\cos\alpha + \frac{1}{2}c_3\sin\beta\cos\beta\Big)\Big] - PL\Big[\frac{1}{2}u_1^2 + \frac{1}{2}u_2^2\Big] \end{aligned} \tag{40}$$

as a truncated Taylor expansion. For simplification, we now suppose $c_2\sin\alpha\cos\alpha = c_3\sin\beta\cos\beta$. Then

$$\begin{aligned} V(u_1, u_2, P) = L^2\Big[&u_1^2\Big(\frac{1}{4}c_2\sin^2\alpha + \frac{1}{4}c_3\sin^2\beta\Big) + u_2^2\Big(\frac{1}{4}c_1 + \frac{1}{4}c_2\cos^2\alpha + \frac{1}{4}c_3\cos^2\beta\Big) \\ &+ u_1^3\Big(\frac{1}{8}c_2\sin^3\alpha - \frac{1}{8}c_3\sin^3\beta\Big) + u_1^2u_2\Big(\frac{3}{8}c_2\sin^2\alpha\cos\alpha + \frac{3}{8}c_3\sin^2\beta\cos\beta\Big) \\ &+ u_1u_2^2\Big(\frac{3}{8}c_2\sin\alpha\cos^2\alpha - \frac{3}{8}c_3\sin\beta\cos^2\beta\Big) + u_2^3\Big(\frac{1}{8}c_1 + \frac{1}{8}c_2\cos^3\alpha + \frac{1}{8}c_3\cos^3\beta\Big) \\ &- u_1^0u_1\Big(\frac{1}{2}c_2\sin^2\alpha + \frac{1}{2}c_3\sin^2\beta\Big) - u_2^0u_2\Big(\frac{1}{2}c_1 + \frac{1}{2}c_2\cos^2\alpha + \frac{1}{2}c_3\cos^2\beta\Big)\Big] \\ &- PL\Big[\frac{1}{2}u_1^2 + \frac{1}{2}u_2^2\Big]. \end{aligned} \tag{41}$$

The generalised co-ordinates are thus diagonalised.

Considering the perfect system for which $u_1^0 = u_2^0 = 0$, the equilibrium conditions $V_1 = V_2 = 0$ show that $u_1 = u_2 = 0$ is the trivial fundamental path.

$$V_{11} = L^2\left[\frac{1}{2}c_2\sin^2\alpha + \frac{1}{2}c_3\sin^2\beta + \frac{3}{4}(c_2\sin^3\alpha - c_3\sin^3\beta)u_1 + \frac{3}{4}(c_2\sin^2\alpha\cos\alpha + c_3\sin^2\beta\cos\beta)u_2\right] - PL$$

and

$$V_{22} = L^2\left[\frac{1}{2}c_1 + \frac{1}{2}c_2\cos^2\alpha + \frac{1}{2}c_3\cos^2\beta + \frac{3}{4}(c_2\sin\alpha\cos^2\alpha - c_3\sin\beta\cos^2\beta)u_1 + \frac{3}{4}(c_1 + c_2\cos^3\alpha + c_3\cos^3\beta)u_2\right] - PL.$$

Hence, the critical loads in the two modes on the fundamental path are given by

$$P_1^c = L\left[\frac{1}{2}c_2\sin^2\alpha + \frac{1}{2}c_3\sin^2\beta\right]$$
$$P_2^c = L\left[\frac{1}{2}c_1 + \frac{1}{2}c_2\cos^2\alpha + \frac{1}{2}c_3\cos^2\beta\right].$$

For a compound critical point $P_1^c = P_2^c = P^c$ so we obtain

$$c_1 = c_2(\sin^2\alpha - \cos^2\alpha) + c_3(\sin^3\beta - \cos^2\beta). \tag{42}$$

Under (42) with $\sin 2\beta \neq 0$, after setting $P = P^c + \lambda$, we see that

$$V(u_1, u_2, \lambda) = -\frac{1}{2}L\lambda(u_1^2 + u_2^2) + \frac{c_2L^2}{8}\left[\frac{\sin\alpha(\sin^2\alpha\cos\beta - \sin^2\beta\cos\alpha)}{\cos\beta}u_1^3 + 3\sin\alpha\cos\alpha(\sin\alpha + \sin\beta)u_1^2u_2 + 3\sin\alpha\cos\alpha(\cos\alpha - \cos\beta)u_1u_2^2 + \frac{(\sin^2\alpha\sin\beta\cos\beta + \sin^2\beta\sin\alpha\cos\alpha - \cos^2\beta\sin\alpha\cos\alpha - \cos^2\alpha\sin\beta\cos\beta + \cos^3\alpha\sin\beta\cos\beta + \cos^3\beta\sin\alpha\cos\alpha)}{\sin\beta\cos\beta}u_2^3\right] + \epsilon_1u_1 + \epsilon_2u_2. \tag{43}$$

It can be seen that u_1 and u_2 are normalised co-ordinates and that (43) is in the form (5), with

$$\epsilon_1 = -\frac{1}{2}\left(\sin^2\alpha + \frac{\sin\beta\sin\alpha\cos\alpha}{\cos\beta}\right)u_1^0, \quad \epsilon_2 = -\frac{1}{2}\left(\sin^2\alpha + \frac{\sin\beta\sin\alpha\cos\alpha}{\cos\beta}\right)u_2^0.$$

We note that when $\alpha = \beta$ the potential function (43) becomes semi-symmetric and we have the model discussed by Thompson and Gaspar. We consider the application of the results of Section 5 to the potential function (43) for different values of α and β. We begin with values which make the potential semi-symmetric.

Case 1. $\alpha = \beta = 105°$

We know, from [8], that the potential function is of anticlinal type.

$C(\theta) = -1.449\cos^2\theta\sin\theta + 1.697\sin^3\theta$.

Solutions of the corresponding eqn (3) are $m = \infty, \pm 0.4259$. These give rise to roots $\theta = (\pi/2)$, $(3\pi/2)$, 0.4026, 3.544, 2.739 and 5.881 of $D(\theta)$.

$E(\theta) = 7.079\sin 3\theta - 0.9105\sin\theta$.

$C(\pi/2) = 1.697$, $C(3\pi/2) = -1.697$, $C(0.4026) = C(2.739) = -0.3785$, $C(3.544) = C(5.881) = 0.3785$.

$E(\pi/2) = -7.9890$, $E(3\pi/2) = 7.9890$, $E(0.4026) = E(2.739) = 6.261$, $E(3.544) = E(5.881) = -6.261$.

The global minimum of $C(\theta)$ occurs at $\theta = (3\pi/2)$ and the perfect path of greatest slope is in the plane of symmetry. The imperfect path with this value of θ and $q = 1$ gives rise to the lowest limit point failure load $\lambda_L^* = -4.513\epsilon^{1/2}$. There are further losses of stability by limit point on the

imperfect paths given by $\theta = 0.4026$ and 2.739 with $q = 1$ since (III) applies, but no initial losses of stability by bifurcation. For $\theta = (\pi/2)$, 3.544 and 5.881 (II) applies so there is an initial bifurcation on the imperfect paths with these θ-values and $q = 1$. Equation (26) shows these occur for negative λ.

The imperfect path given by $\theta = (\pi/2)$ and $q = 1$ has the bifurcation failure load $\lambda_B = -1.025\epsilon^{1/2}$, that by $\theta = 3.544$ or 5.881 and $q = 1$ has the bifurcation failure load $\lambda_B = -2.048\epsilon^{1/2}$.

Case 2. $\alpha = \beta = 130°$

We know, from [8], that the potential is of homeoclinal type.

$$C(\theta) = -2.263\cos^2\theta\sin\theta - 0.9194\sin^3\theta.$$

Solutions of $D(\theta)$ are $\theta = (\pi/2), (3\pi/2), 0.8470, 3.9890, 2.2946$ and 5.4362.

$$E(\theta) = 3.023\sin 3\theta - 1.2553\sin\theta.$$

$C(\pi/2) = -0.9194$, $C(3\pi/2) = 0.9194$, $C(0.8470) = C(2.2946) = -1.130$, $C(3.9890) = C(5.4362) = 1.130$.

$E(\pi/2) = -4.2783$, $E(3\pi/2) = 4.2783$, $E(0.8470) = E(2.2946) = 0.7678$, $E(3.9890) = E(5.4362) = -0.7678$.

The global minimum of $C(\theta)$ occurs at $\theta = 0.8470$ and 2.2946. The perfect paths of greatest slope correspond to these values of θ so equation (26) with these θ-values and $q = 1$ gives the imperfect path with the lowest limit point failure load $\lambda_L^* = -3.682\epsilon^{1/2}$. The paths given by equation (26) and $\theta = 3.9890$ or 5.4362 do not have a limit point by (II). If $q = 1$, there is an initial bifurcation on these paths but (26) shows it occurs for positive λ. By (IV) there is both a limit point and bifurcation on the path given by eqn (26) with $\theta = (\pi/2)$ and $q = 1$. Using results (35) and (36) we deduce that $r_B < r_L$ so that the bifurcation is initial. Equation (26) shows that $\lambda_B = -3.395\epsilon^{1/2}$. The worst failure is again as predicted by Ho.

We now look at two examples of a general cubic potential.

Case 3. $\alpha = 45°$, $\beta = 60°$

$$C(\theta) = -0.3964\cos^3\theta + 2.360\cos^2\theta\sin\theta + 0.3107\cos\theta\sin^2\theta + 1.075\sin^3\theta.$$

It is easily checked that the corresponding cubic has positive discriminant so that the cubic part of the potential has one real root, see [3]. The corresponding cubic (3) is

$$0.3107m^3 + 1.495m^2 - 1.8106m - 2.36 = 0. \tag{44}$$

We may check that this has negative discriminant and hence that it has three real roots. Following [3], this general cubic potential is of homeoclinal type. We show, in the appendix, how this agrees with the semi-symmetric definition of Thompson and Hunt.

Solving (44) by a standard method we find $m = 1.6276, -5.6089, -0.8313$. Corresponding solutions of $D(\theta)$ are

$$\theta = 1.0199, 4.1614, 1.7472, 4.8888, 2.4480 \text{ and } 5.5896.$$

Using (31) and (32).

$$C(\theta) = -0.1768\cos 3\theta + 0.3213\sin 3\theta - 0.2196\cos\theta + 1.3963\sin\theta.$$

$$E(\theta) = 1.5901\cos 3\theta - 2.8913\sin 3\theta + 0.2196\cos\theta - 1.3963\sin\theta.$$

$C(1.0199) = 1.2772$, $C(4.1614) = -1.2772$, $C(1.7472) = 1.0466$, $C(4.888) = -1.0466$, $C(2.448) = 1.2556$, $C(5.5896) = -1.2556$.

$E(1.0199) = -2.897$, $E(4.1614) = 2.897$, $E(1.7472) = 1.886$, $E(4.888) = -1.886$, $E(2.448) = -2.808$, $E(5.5896) = 2.808$.

The global minimum of $C(\theta)$ and the perfect path of greatest slope occur when $\theta = 4.1614$. Equation (26) with $\theta = 4.1614$ and $q = 1$ gives the imperfect path with the lowest limit point failure load $\lambda_L^* = -3.915\epsilon^{1/2}$. By (II), the imperfect paths given by (26) with $\theta = 1.0199$ or 2.448 and $q = 1$ have an initial bifurcation but this occurs for positive λ. By (I), the imperfect path given by (26) with $\theta = 1.7472$ and $q = 0$ has an initial bifurcation for positive λ, while by (III) the path given by (26) with $\theta = 5.5896$ has an initial failure by limit point for negative λ. Using (IV), we find that the imperfect path given by $\theta = 4.8888$ and $q = 1$ has both a limit point and bifurcation for negative λ. From (35) and (36) we find that $r_L < r_B$ so that initial failure is by limit point. The imperfect paths are shown in Fig. 2. As all negative initial failure loads are by limit point Ho's result is again illustrated.

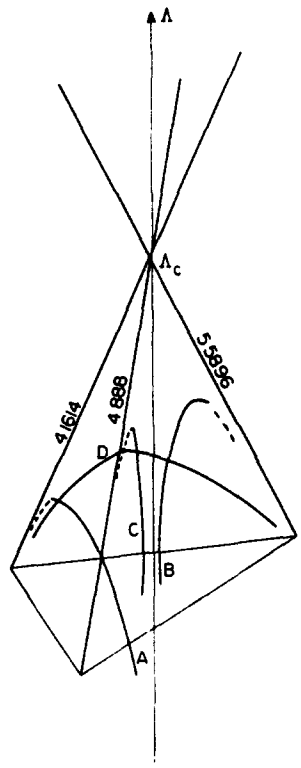

Fig. 2. Imperfect paths exhibiting instability for negative λ. Paths *A* and *B*, corresponding to $\theta = 4.1614$ and 5.5896 become unstable at a limit point and path *C*, corresponding to $\theta = 4.888$, also becomes unstable at a limit point but experiences a secondary bifurcation with a path in the plane of the other two perfect paths.

Case 4. $\alpha = 45°$, $\beta = 120°$

The cubic part of the potential (43) is

$$1.1036u_1^3 + 2.36u_1^2u_2 + 1.811u_1u_2^2 + 0.0795u_2^3$$

It is easily shown that this has positive discriminant so that it has one real root. The corresponding eqn (3) is

$$1.811m^3 + 4.4815m^2 - 0.3112m - 2.36 = 0. \tag{45}$$

This cubic has negative discriminant and hence three real roots. Following [3] and the appendix, our general cubic potential is of homeoclinal type.

Solving (45) we find $m = 0.6715, -2.3036, -0.8424$, yielding roots $\theta = 0.5914, 3.7329, 1.9804, 5.1219, 2.4415$ and 5.5831 of $D(\theta)$.

Using (31) and (32),

$$C(\theta) = -0.1768\cos 3\theta + 0.5701\sin 3\theta + 1.2805\cos\theta + 0.6496\sin\theta.$$

$$E(\theta) = 1.5917\cos 3\theta - 5.1311\sin 3\theta - 1.2805\cos\theta - 0.6496\sin\theta.$$

$C(0.5914) = 2.0193$, $C(3.7329) = -2.0193$, $C(1.9804) = -0.2719$, $C(5.1219) = 0.2719$, $C(2.4415) = -0.1580$, $C(5.5831) = 0.1580$.

$E(0.5914) = -6.7720$, $E(3.7329) = 6.7720$, $E(1.9804) = 3.1343$, $E(5.1219) = -3.1343$, $E(2.4415) = -3.0638$, $E(5.5831) = 3.0638$.

The global minimum of $C(\theta)$ occurs when $\theta = 3.7329$. The worst limit point failure load occurs on a path (26) with $\theta = 3.7329$ and $q = 1$ and is given by $\lambda_L^* = -4.923\epsilon^{1/2}$. A further use of (III) shows that there is an initial limit point failure on the imperfect path given by (26) with $\theta = 1.9804$ and $q = 1$ for negative λ. The imperfect path given by (26) with $\theta = 5.5831$ and $q = 0$ is covered by (I) and there are no limit points or bifurcations on it for negative λ. Two of the remaining imperfect paths of the type (26) are covered by (II), when $\theta = 0.5914$ and 5.1219 with $q = 1$. There is no limit point but an initial bifurcation on each for negative λ. For $\theta = 0.5914$, $\lambda_B = -0.2744\epsilon^{1/2}$ while for $\theta = 5.1219$, $\lambda_B = -1.310$. There remains $\theta = 2.4415$ which is covered

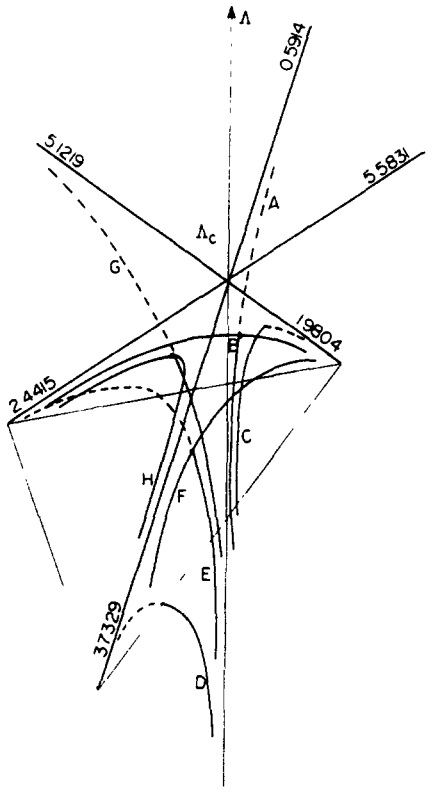

Fig. 3. Imperfect paths exhibiting instability for negative λ. Path A, corresponding to $\theta = 0.5914$, becomes unstable at a bifurcation with the path B in the plane of the other two perfect paths. Paths C and D show failure by limit point, the latter having the lowest failure load for fixed magnitude of imperfection. Path E, corresponding to $\theta = 2.4415$, becomes unstable at a bifurcation with the path F in the plane of the other two perfect paths. There is a secondary limit point on path E. Path G, corresponding to $\theta = 5.1219$, becomes unstable at a bifurcation with path H in the plane of the other two perfect paths.

by (IV). The corresponding imperfect path given by (26) and $q = 1$ has both a limit point and bifurcation for negative λ. Results (35) and (36) show that $r_B < r_L$ and hence initial failure is by bifurcation. The important imperfect paths are shown in Fig. 3. From (26) we find $\lambda_B = -2.021\epsilon^{1/2}$. Ho's theorem is again illustrated.

7. AN INTUITIVE PROOF OF HO'S THEOREM

Ho's theorem

For the cubic type discussed here and a fixed magnitude ϵ of the imperfection vector, the lowest failure load producing an initial loss of stability occurs when the vector is in the direction of the perfect path of greatest slope. Further, it always occurs at a limit point.

Our proof follows naturally from the observations (I)–(IV) made so far and the expression of $C(\theta)$ and $E(\theta)$ as trigonometric polynomials. We require

Bernstein's theorem

If $T(\theta)$ is a trigonometric polynomial of degree n then

$$|T'(\theta)| \leq n \cdot \max |T(\theta)|.$$

A proof may be found in Zygmund's book [6], or in Bary's book[7].

It follows immediately from Bernstein's theorem that

$$|E(\theta)| \leq 9|C(\theta_{m^*}^{n^*})| \tag{37}$$

Proof of Ho's theorem

We already know that the lowest limit load occurs when the imperfection is in the direction of the perfect path of steepest descent and that this does represent an initial loss of stability. By (I)–(IV) we need only compare this lowest limit load with bifurcations of types (II) and (IV).

We consider first a bifurcation of type (II). Here, $C(\theta_n^m)>0$ and $E(\theta_n^m)<0$ while $q=1$. By (26)

$$\lambda=\epsilon^{1/2}\left\{\frac{3C(\theta_n^m)}{[-E(\theta_n^m)]^{1/2}}-[-E(\theta_n^m)]^{1/2}\right\}=\epsilon^{1/2}\left\{\frac{3C(\theta_n^m)+E(\theta_n^m)}{[-E(\theta_n^m)]^{1/2}}\right\}.$$

The assumption that λ is negative implies $-E(\theta_n^m)>3C(\theta_n^m)$.

$$\begin{aligned}
\lambda^2&=\frac{\epsilon}{-E(\theta_n^m)}\{9C^2(\theta_n^m)+6C(\theta_n^m)E(\theta_n^m)+E^2(\theta_n^m)\}=\epsilon\left\{\frac{9C^2(\theta_n^m)}{-E(\theta_n^m)}-6C(\theta_n^m)-E(\theta_n^m)\right\}\\
&<\epsilon\left\{\frac{9C^2(\theta_n^m)}{3C(\theta_n^m)}-6C(\theta_n^m)-E(\theta_n^m)\right\}=\epsilon\{-3C(\theta_n^m)-E(\theta_n^m)\}\\
&<-\epsilon E(\theta_n^m)\\
&<-\epsilon 9C(\theta_{n*}^{m*}) \quad \text{by (37)}\\
&<-\epsilon 12C(\theta_{n*}^{m*})\\
&=\lambda_L^{*2}.
\end{aligned}$$

We now consider a bifurcation arising from case (IV), when it produces the initial stability loss on a path also containing a limit point. $C(\theta_n^m)$ and $E(\theta_n^m)$ are both negative with $q=1$, while we must have $|E(\theta_n^m)|>3|C(\theta_n^m)|$. By (26)

$$\begin{aligned}
\lambda&=\epsilon^{1/2}\left\{\frac{3C(\theta_n^m)}{[-E(\theta_n^m)]^{1/2}}-[-E(\theta_n^m)]^{1/2}\right\}\\
\lambda^2&=\epsilon\left\{\frac{9C^2(\theta_n^m)}{-E(\theta_n^m)}-6C(\theta_n^m)-E(\theta_n^m)\right\}\\
&<\epsilon\left\{\frac{9C^2(\theta_n^m)}{3C(\theta_n^m)}-6C(\theta_n^m)-E(\theta_n^m)\right\}\\
&=\epsilon\{-3C(\theta_n^m)-E(\theta_n^m)\}\\
&\leqslant\epsilon\{-3C(\theta_{n*}^{m*})-9C(\theta_{n*}^{m*})\} \quad \text{by (37)}\\
&=-\epsilon 12C(\theta_{n*}^{m*})\\
&=\lambda_L^{*2}.
\end{aligned}$$

These two results prove Ho's theorem.

Acknowledgement—I would like to express my thanks to Professor Michael Thompson for several helpful discussions.

REFERENCES

1. J. M. T. Thompson and G. W. Hunt, Towards a unified bifurcation theory. *J. Appl. Math. Phys. Z.A.M.P.*, **26** 581–603 (1975).
2. G. W. Hunt, Imperfection sensitivity of semi-symmetric branching. *Proc. Roy. Soc. Lond. A.* **357**, 193–211 (1977).
3. P. Samuels, The relationship between post-buckling behaviour at coincident branching points and the geometry of an umbilic point of the energy surface. *J. Structural Mech.* **7**(3), 297–324 (1979).
4. D. Ho, Buckling load of non-linear systems with multiple eigenvalues . *Int. J. Solids Structures* **10**, 1315–1330 (1974).
5. J. M. T. Thompson, J. K. Y. Tan and K. C. Lim, On the topological classification of post-buckling phenomena. *J. Structural Mech.* **6**, 383–414 (1978).
6. A. Zygmund, Trigonometric series. Cambridge (1968).
7. N. K. Bary, *A Treatise on Trigonometric Series.* Vol. 1. Pergamon, Oxford (1964).
8. J. M. T. Thompson and Z. Gaspar, A buckling model for the set of umbilic catastrophes. *Math. Proc. Camb. Phil. Soc.* **82**, 497–507 (1977).

APPENDIX

Following [3], a general cubic potential is anticlinal if its cubic part and hence (3), has three real roots and homeoclinal if its cubic part has one real root and eqn (3) three real roots. Clearly, for an anticlinal potential $C(\theta)$ and $D(\theta)$ both have six real roots while for a homeoclinal potential $C(\theta)$ has two real roots and $D(\theta)$ six.

The semi-symmetric view of Thompson and Hunt is that an anticlinal potential has the symmetric projection of the two coupled paths falling in the direction opposite to that of the uncoupled path while a homeoclinal potential has them falling in the same direction.

We point out that the general algebraic definition in [3], for the three path cases, can be interpreted in a manner akin to that of Thompson and Hunt.

Let $\theta_1^1, \theta_2^1, \theta_3^1, \theta_1^2, \theta_2^2, \theta_3^2$ be the six roots of (23) occurring in the interval $0 \leqslant \theta < 2\pi$ in order of magnitude, where $\tan \theta_n^m = m_n$, $n = 1, 2, 3$, $m = 1, 2$. As $\theta_n^2 = \theta_n^1 + \pi$ any three consecutive θ_n^m lie within a range of π. We also recall from (24) that $C(\theta_n^m)$ is one third of the slope in the $r\lambda$-plane of the post-buckling path with $\theta = \theta_n^m$ and starting at the origin. We list the range of possibilities for the signs of $C(\theta_n^m)$.

θ	$C(\theta)$							
θ_1^1	−	+	−	+	−	+	−	+
θ_2^1	+	−	−	+	−	+	+	−
θ_3^1	−	+	−	+	+	−	+	−
θ_1^2	+	−	+	−	+	−	+	−
θ_2^2	−	+	+	−	+	−	−	+
θ_3^2	+	−	+	−	−	+	−	+
$\theta_1^1 + 2\pi$	−	+	−	+	−	+	−	+
	Case (a)	Case (b)	Case (c)	Case (d)	Case (e)	Case (f)	Case (g)	Case (h)

There can be no further changes of sign of $C(\theta)$ between consecutive θ_n^m-values as there would have to be an even number of them and hence there would be a solution of (23) between consecutive θ_n^m-values, a contradiction.

It follows that cases (a) and (b) provide six roots of $C(\theta)$ in an interval of length 2π and hence correspond to an anticlinal potential while the remaining cases provide only two roots of $C(\theta)$ in an interval of length 2π and correspond to a homeoclinal potential.

We hence see that for a homeoclinal potential we can find three *consecutive* paths falling in the same direction with respect to the λ-axis, either all above the $r\theta$-plane or all below. For the anticlinal potential we cannot even find two consecutive paths falling in the same direction with respect to the λ-axis.